Visualization and characterization of localized outgassing position on surface-treated specimens: chromium oxide layer on stainless steel

Naoya Miyauchi[a], Tomoya Iwasawa[a,b], Taro Yakabe[a], Masahiro Tosa[a], Toyohiko Shindo[c], Shoji Takagi[d], and Akiko N. Itakura[a]

[a] *National Institute for Materials Science, 1-2-1 Sengen, Tsukuba, Ibaraki 305-0047, Japan*

[b] *University of Tsukuba, 1-1-1 Tennodai, Tsukuba, Ibaraki 305-8577, Japan*

[c] *Contamination Control Services Inc., 529-3 Shimokuzawa, Midori-ku, Sagamihara, Kanagawa 252-0134, Japan*

[d] *Toho University, 2-2-1 Miyama, Funabashi, Chiba 274-8510, Japan*

Abstract

Hydrogen outgassing from a metal surface and a coated metal surface was visualized by two-dimensional mapping of hydrogen ions desorbed upon scanning electron beam irradiation. The samples used were stainless steel covered with a dense chromium oxide layer, and a reference surface of stainless steel. The coating layer was made by using the segregation phenomenon of the metal. Outgassing of hydrogen was detected from the holelike defects on the treated surface. However, hydrogen was not released from all the holelike defects seen in the SEM image. The outgassing positions were positions without chromium, but not all areas without chromium and/or oxygen coincided with outgassing positions.

KEYWORDS: hydrogen diffusion, desorption, surface segregation

Corresponding author
E-mail address: MIYAUCHI.Naoya@nims.go.jp
Postal address: National Institute for Materials Science, 1-2-1 Sengen, Tsukuba, Ibaraki 305-0047, Japan

1. Introduction

There are several different types of surface treatment, each applicable to different kinds of devices [1-3]. The surface coatings for vacuum systems include water-barrier films and hydrogen-barrier films. To assess the effectiveness of these surface treatment, as polishing or coatings, the degree of outgassing from the surface during evacuation is determined by reducing the ultimate pressure in a chamber or by direct measurement of the total amount of gas desorption in a vacuum gauge or quadrupole mass spectrometer by a thermal desorption method. However, the more perfect the coating film, the less the amount of released gas, making it increasingly difficult to detect. In addition, it takes a long time for gas to pass through a good barrier film, and the transmission signal is often eclipsed by gas molecules from the background.

We have developed an *operando* hydrogen microscope that enables the direct detection of adsorbed hydrogen on a surface by utilizing the electron-stimulated desorption (ESD) with hydrogen supplied at various temperatures [4,5]. In principle, this instrument is also capable of detecting other kinds of electron-excited atoms. The atoms and molecules detected are those originally adsorbed from the gas-phase space existing on a sample and those diffusing out from the sample material. It is possible to use the *operando* hydrogen microscope to measure the properties of a treated surface with respect to its vacuum and/or barrier effect together with the position information of the existing hydrogen. In addition, by using the *operando* hydrogen microscope, it is possible to compare two different surfaces in one image under the same vacuum environment and measurement conditions, in real time. In the current study, we used this instrument to evaluate the effects of treatment by the Fe-free super passivation process (FF-SPP), which was developed to create anticorrosion, low-adsorption surfaces [6]. We formed a Cr_2O_3 layer by the FF-SPP, that is, a cycle of heating and acid rinsing. The Cr was segregated from SUS316L by heat treatment, and Cr_2O_3 was formed from the segregated Cr and oxygen in air. The thickness of the Cr_2O_3 layer can be roughly controlled to around 2 nm to 5 nm by adjusting the treatment temperature and the heating cycle, but the uniformity and reproducibility were poor. We have already reported that FF-SPP–treated surfaces have a low rate of hydrogen outgassing compared with electropolished (EP) surfaces [6]. In this

study, we will go one step further and examine the locations where the amounts of local outgassing of hydrogen are high.

2. Experimental

2.1. Sample preparation by FF-SPP processing

The specimens used for FF-SPP processing were stainless steel (SUS 316L steel). The FF-SPP involved first electropolishing the surface of the steel specimens and then heat treatment after washing with organic solvent and mixed acid. The heat treatment was carried out by holding the specimen in the air at a set temperature, followed by washing with the mixed acid solution to remove surface iron, and heat treatment again at a temperature lower than the initial set temperature. Since the details of the fabrication of the dense chromium oxide layer by the FF-SPP belong to Contamination Control Services Inc., they are not given here. We previously reported that the outgassing rate of a vacuum vessel with an FF-SPP-treated inner surface was lower than that of a vacuum vessel that was only electropolished. In particular, within 5 to 10 min of starting vacuum evacuation, the FF-SPP–treated vessel reached an outgassing rate that was the same as that of the electro-polished vessel evacuated for 120 min [6].

2.2. Surface analysis and profiling (AES and GDOES)

In the current study, we used two samples (samples No. 1 and No. 2) of electropolished stainless steel of the same composition (SUS 316L). The FF-SPP was applied only to sample No. 1 to distinguish the effect of the FF-SPP, using sample No. 2 with only electropolishing as a reference. Surface analysis was performed by scanning Auger electron spectroscopy (AES; SAM 660, ULVAC-PHI, Chigasaki, Japan) at an incident energy of 5 keV and an incident current density of 50 nA/mm^2. The spatial resolution under this condition is 1 μm. However, under these conditions, the amount of deposited carbon originating from inside the film during measurement cannot be ignored, so it is used only to confirm the atomic species constituting the outermost surface. For the elemental analysis in the depth direction, we adopted glow discharge optical emission spectrometry (GDOES; GD-Profiler2, Horiba). GDOES involves sputtering the atoms constituting the surface with Ar plasma and measuring the emission spectrum. From argon plasma, Ar^+ ions with incidence

energy of 50 eV and current of 1000 A/m^2 irradiate the sample. Under these conditions, the analysis speed of the depth profiling is 7.5 nm/s. A fine shadow effect is expected to be present, and the substantial area involved in the analysis is considered to be average, since the surface of the sample has an unevenness of several nm owing to the effects of acid treatment and heat treatment. The measured elements are the main components of stainless steel, such as iron (Fe), chromium (Cr), nickel (Ni), oxygen (O), carbon (C), and elements contained in trace amounts in steel. We confirmed the presence of sulfur (S), molybdenum (Mo), phosphorus (P), manganese (Mn), and hydrogen (H), which are elements that may easily be contaminants from the holder.

2.3. Operando hydrogen microscope and the mechanism of desorption induced by electronic transition.

ESD is a powerful investigative tool for surface analysis, wherein electrons are utilized to stimulate the excitation of the bonding state between adsorbed atoms and the surface. From here on, we refer to ESD as "desorption induced by electronic transitions (DIET)" to highlight the desorption mechanism involved in ESD. Ions desorbed by DIET contain a large amount of information relevant to the study of the bonding and dynamical behaviors of species chemisorbed on a surface. In addition, the DIET technique has been shown to perform well in detecting the distribution of hydrogen on a surface [7]. Our *operando* hydrogen microscope is a device incorporating a DIET measurement system in a scanning electron microscope (SEM), allowing images of hydrogen on the sample surface to be measured with high resolution. It is also possible to carry out measurements over a long period of time while supplying hydrogen from the back of the sample. In the current study, we performed these measurements using hydrogen inherent in the stainless-steel sample. Secondary electron images and hydrogen DIET images were taken at an electron acceleration energy of 3 keV. To compare the two samples under the same conditions and in the same image, sample No. 1 with the FF-SPP–treated surface and sample No. 2 with the electropolished surface were fixed side-by-side in the sample holder. Therefore, in the SEM images, a gap can be seen between the two samples. The base pressure of 1.0×10^{-7} Pa for DIET measurement was achieved by baking the

ultrahigh-vacuum (UHV) chamber at 403 K for 24 h. The gas component in the chamber was measured with a quadrupole mass spectrometer (QMG220; Pfeiffer, Aslar, Germany). The main residual gas at room temperature was hydrogen. The background pressure during the DIET experiment was lower than 5.0×10^{-7} Pa, as monitored with an ion gauge together with component measurement with the quadrupole mass spectrometer. The sample temperature was raised to 473 K for DIET measurement. We found that hydrogen was the main component of outgassing at this temperature (Fig. 1) and included that outgassed from the sample, sample holder, and the inside of the equipment. The mass number of ions at m/z = 1 and 2 increased and became conspicuously large when the sample was heated. We consider the DIET ions desorbed from the sample surface to be mainly hydrogen ions.

3. Results and discussion

3.1. Hydrogen mapping of FF-SPP surface and electropolished surface

Figure 2 shows SEM images and DIET measurements of the FF-SPP–treated and electropolished surfaces. By comparing the DIET maps showing ion desorption of samples No. 1 and No. 2, we found that the FF-SPP surface treatment lowered hydrogen desorption more than electropolishing alone. Two red spots were also detected in the DIET image. They coincided with two of the holelike defects seen in the SEM image. We carefully compared these large desorption points in the DIET map with the SEM image. From the SEM image, it was confirmed that there are holelike defects on the edges of both samples (indicated by arrows 1–4 on sample No. 1, which was the FF-SPP–treated surface, and arrows 5–7 on sample No. 2, which was the electropolished surface), but from the SEM image, it cannot be judged whether these are impurities or defects (e.g., cavities or irregularities). The size of the defect in the SEM image was unrelated to the degree of ion emission in the DIET image; only the positions of two defects, numbers 1 and 3, showed significant desorption peaks in the DIET image. The positions of defects 5–7 did not show any visible peaks in the DIET images. These results indicate that a large amount of gas was emitted at the points of only two holelike defects on the FF-SPP–treated surface. From the hydrogen diffusion profile along line A–B (Fig. 2d), it can be seen that the area subjected to the FF-SPP process (left side of the image)

has lower ion desorption than the area subjected to electropolishing alone. By careful observation, we found that the defective part of EP shows more outgassing than other parts of EP, but the amount of local outgassing was only 20–30% higher than the mean value of EP outgassing. On average, the amount of desorption was reduced by FF-SPP treatment to about one-third of that with electro-polishing alone. From the profile along line C–D, we can see that more than 30 times as many ions were desorbed from the position of the holelike defect as from other points on the FF-SPP–treated surface. Although the defect was in the FF-SPP–treated area, desorption from the defect position was greater than the amount of ion desorption from any point on the surface treated by electropolishing alone. It is suspected that the contamination on the surface may result in the origin source of the outgassing.

3.2. AES mapping of FF-SPP surface and electropolished surface

Figure 3 shows the distribution of surface atoms measured by AES. AES mapping of the same samples was carried out after DIET measurement. The Auger electron energies of each map were 269.5 eV for carbon, 702.5 eV for iron, 527.0 eV for chromium, and 509.0 eV for oxygen. The FF-SPP–treated sample and the electropolished sample were arranged side-by-side in the sample holder in the AES machine, similarly to the arrangement for DIET measurements. However, in fact, the samples were slightly displaced in the left–right direction (Fig. 3a). We discovered this because the area of carbon-based contaminants was shifted slightly (Fig. 3c). The area indicated by the dotted line in Fig. 3c should have been the irradiated area during the DIET measurement. It is well known empirically that the carbon peak increases under electron irradiation, and carbon-based contaminants would have been adsorbed during electron irradiation for the DIET measurements. In this area, the carbon peak was increased by the >20 h electron irradiation for DIET measurement. The carbon on the surface was removed by sputtering with low-energy argon ions of 1 keV for 20 s. Figs. 3c to 3f show the surfaces before carbon removal; Figs. 3g to 3j show the surfaces after carbon removal. For the sputtering, the samples were tilted at 30 degree toward the ion gun, taking care not to shift the measurement position of the sample. Therefore, the vertical direction of the 3g-3j AES map appears in the image as short as about 87% as compared to 3c-3f, while the horizontal direction is the same

scale for all the AES images. Since the beam of argon ions strikes the samples at an oblique angle, the side surface of the sample is not irradiated and some carbon remains (3g). Oxygen is present only on the FF-SPP–treated sample (chromium oxide side). Chromium is present on the FF-SPP–treated sample, but because it exists in the original stainless steel, it can be seen that it also exists on the electropolished sample. As the carbon contamination was removed, a difference in the distributions of iron between the FF-SPP sample and the electropolished sample became apparent. Chromium and oxygen are segregated on the surface of the FF-SPP–treated sample, and the iron peak cannot be seen. Therefore, the surface is coated with Cr_2O_3. On the other hand, the surface of the electropolished sample is covered with iron and chromium, and the oxygen concentration is low. We focused on the two defects (arrows 1 and 3 in Fig. 3b) in the area where DIET measurement was performed. There was no particular bias with respect to oxygen, chromium, nickel, or iron within the measurement sensitivity of AES. In the chromium distribution map, the points marked by arrows showed a smaller signal than the remaining surface of the FF-SPP–treated sample. No decline in chromium was seen at the defect positions other than 1 and 3. Since the amount of chromium on the FF-SPP surface, other than at the defect positions, fluctuates, it cannot be explained from only the AES result. This indicates the possibility of the chromium oxide coating being incomplete at those defects and hydrogen outgassing being increased. On the other hand, we measured the thickness of Cr_2O_3 to be 4 nm by depth profiling in GDOES.

3.3. Models of local outgassing from FF-SPP surface

We consider the phenomenon of hydrogen desorption from the surface of a bulk sample (block) made of metal alloy. It is assumed that the alloy material has a single structure, and is uniform and isotropic. It is also assumed that hydrogen is present in a certain and sufficient amount in the block, and the reduction in the number of hydrogen atoms owing to desorbing emission (or outgassing) has a negligible effect on the amount of hydrogen remaining in the block. When this block material is heated in a vacuum, hydrogen escapes from the surface of the material, and a concentration gradient perpendicular to the surface is formed in the vicinity of the surface (indicated by gray shading in

Fig. 4a). The migration (diffusion) direction of hydrogen under this concentration gradient is from inside the bulk of the material to the surface (as indicated by arrows B → S). Let us now consider the case where a diffusion barrier coating film is present on the surface of the block. Hydrogen can escape only at a defect (opening) in the barrier film. The concentration gradient of hydrogen becomes a concentric spherical gradation centered on the defect (opening). The diffusion of hydrogen here is from around the sphere to its center (as indicated by arrows R → C in Figs. 4b, 4c, and 4d). If it is assumed that hydrogen diffuses as a viscous flow similarly to the flow of a gas in a confined container, the desorption per unit area is considered to be larger than that in Fig. 4a, as schematically shown in Fig. 4b. However, hydrogen in the metal undergoes quantum diffusion [8], and there is no interaction between hydrogen atoms and atoms in the metal alloy. When we use the analogy of a gas flow, it is a molecular flow. In the case of a molecular flow, the amount of released hydrogen is proportional only to the size of the opening (defect in the barrier film). When the behavior of hydrogen is assumed to be a molecular flow, the amount released per unit area is the same as in Fig. 4a, as it is schematically shown in Fig. 4c [9]. However, the concentration gradient is different in the cases of release from the plane and release from one point. In Fick's laws of diffusion, the diffusion flux is proportional to the concentration gradient. Therefore, it is considered that the number of released atoms per unit area is proportional to the concentration gradient. Outgassing should increase with the concentration gradient. The degree of hydrogen desorption per unit area from the opening of the barrier film, as measured by DIET, was more than 30 times that from the noncoated surface. On the basis of these results, we propose the following model. The barrier film of chromium oxide produced by the FF-SPP involves the surface segregation phenomenon; that is, the FF-SPP causes the diffusion of the chromium in the stainless steel to the surface. Oxygen is acquired from the atmosphere during heating in the segregation operation. As a result of the segregation or diffusion of atoms between adjacent materials, an interlayer with different proportions of constituent atoms is formed in the vicinity of the interface. Fig. 4d illustrates this model, in which an interfacial layer with less chromium is formed directly beneath a chromium-rich barrier coating, which is a segregation layer. Compared with the diffusion of hydrogen in

stainless steel, the diffusion coefficient of hydrogen in iron or iron–nickel alloy is large [10]. Hydrogen diffuses through the chromium-depleted intermediate layer and it is conceivable that it is released through the defect in the barrier layer. In other words, the amount of released hydrogen in the model (Fig. 4d) is considered to be the sum of diffused hydrogen in stainless steel (Fig. 4c) and hydrogen diffusing through the intermediate layer formed at the interface. The occurrence of segregation means that a concentration gradient is formed. Therefore, in the vicinity of the interface between the surface of the base material and the base material of the segregation layer, the segregation element should be lower than the solid solution concentration of the base material.[ref][ref] The other possibility is an increase in the "surface" area under the holelike defect (Fig. 4e). We assume a deep well lying under the defect. Hydrogen atoms diffuse from around the metal to the well (as indicated by arrows R → W), through the inside wall of the well. Hydrogen atoms and hydrogen gas, which are formed in a well, flow out through the well and are released from the holelike defect. It is known that stainless steel has small inclusions of precipitated MnS or other sulfides [11]. Steel around the inclusions dissolves more than the steel matrix, resulting in the formation of pits around the inclusions, causing the inclusions around a surface to be peeled off by electropolishing. The size of the well should be the same as that of an inclusion, which is expected to be one reason for the large outgassing from the holelike defect. We believe that with the model described in Figs. 4d and 4e, more robust information can be obtained by carefully analyzing the sample surface in the direction of depth around the defect part. Measurement by GDOES did not identify any chromium-depleted layer, as shown in Fig. 4d, for this sample in the depth direction. In addition, we believe that the difference in the diffusion coefficient of hydrogen can be explained by performing local structural analysis by reflection high-energy electron diffraction (RHEED) or electron backscattering diffraction (EBSD).The remaining problem is the possibility that the amount of hydrogen in the bulk is higher in the FF-SPP sample than in the electropolished one, since the coating layer acts as a diffusion barrier that blocks outgassing from the sample before the experiment. Considering that the Cr_2O_3 coating of the FF-SPP sample is a strong diffusion barrier of hydrogen, it may reduce hydrogen outgassing from the sample. As a result of the small amount of

hydrogen released, it is considered that the hydrogen content of the FF-SPP sample is higher than that of the electropolished one. The higher content hydrogen than EP sample will be released from smaller release sites than EF samples (i.e. only the specific holelike defects). For this reason, outgassing from defects 1 and 3 of the FF-SPP sample may have increased. ~~There is also a possibility that outgassing from defects 1 and 3 of the FF-SPP sample increases.~~

4. Conclusion

We used an *operando* hydrogen microscope to evaluate barrier films used for surface modification. Multiple samples were compared in one field of view, and the effect of the barrier film was confirmed. Hydrogen release from a small defect could be detected. In the study of barrier films, a higher barrier effect was expected upon eliminating these defective areas. We confirmed the effectiveness of using the *operando* hydrogen microscope for evaluating surface modifications and barrier films.

Acknowledgments

We thank Mr. A. Kasahara of National Institute for Materials Science (NIMS) and Mr. S. Nakamura of Toho University for their help with our experiment. We thank Dr. M. Yoshitake of NIMS and Mr. T. Miyata of Shinwa Vanes Co. Ltd. for their helpful discussion. We thank Dr. T. Moriyama and Mr. A. Fujimoto of Horiba Techno Service Co. Ltd. for the GDOES measurement and discussion. This research was supported by MEXT/JSPS KAKENHI Grant Number JP 18H03849 and the joint research fund from Shinwa Vanes Co. Ltd.

References

[1] Y. Ishikawa and V. Nemanic, An overview of methods to suppress hydrogen outgassing rate from austenitic stainless steel with reference to UHV and EXV, Vacuum **69** (2003) 501–512.

[2] A. Itakura, M. Tosa, S. Ikeda and K. Yoshihara, Hydrogen permeation properties and surface structure of BN-coated stainless steel membrane, Vacuum **47** (1996) 697–700.

[3] S. Tsukahara, S. Inayoshi, Y. Ootsuka, S. Misawa and A. Tanaka, Outgassing Rate and Morphology of Surface Oxide Layer of Aluminum Alloy for Vacuum Equipment Use, Journal of Vacuum Society Japan **43** (2000) 209–213.

[4] N. Miyauchi, S. Suzuki, S. Takagi, T. Gotoh, Y. Murase and A. N. Itakura, Electron Stimulated Desorption Measurement of Permeated Hydrogen through

Stainless Steel Membrane, Journal of Vacuum Society Japan **58** (2015) 387–391.

[5] N. Miyauchi, K. Hirata, Y. Murase, H. A. Sakaue, T. Yakabe, A. N. Itakura, T. Gotoh and S. Takagi, 2D mapping of hydrogen permeation from a stainless steel membrane , Scripta Materialia **144** (2018) 69–73.

[6] A. N. Itakura, M. Tosa, T. Yakabe, N. Miyauchi, A. Kasahara, T. Miyata and T. Shindo, Low Outgas Surface Treatment of Stainless Steel 316L Using Segregated Chromium Oxide Layer, Vacuum and Surface Science **61** (2018) 675–680.

[7] Y. Itoh and K. Ueda, Hydrogen and oxygen behaviors on Porous-Si surfaces observed using a scanning ESD ion microscope, Applied Surface Science **237** (2004) 596–601.

[8] S. Fujita and A. Garcia, Theory of hydrogen diffusion in metals. Quantum isotope effects, Journal of Physics and Chemistry of Solids **52** (1991) 351–355 (1991).

[9] S. M. Rossnagel, in *Handbook of Vacuum Science and Technology*, edited by D. M. Hoffman, B. Singh and I. J. H. Thomas, High-vacuum-based processes, Academic Press, (1998).

[10] V. Olden, C. Thaulow and R. Johnsen, Modelling of hydrogen diffusion and hydrogen induced cracking in supermartensitic and duplex stainless steels, Materials and Design **29** (2008)1934.

[11] A. Chiba, I. Muto, Y. Sugawara and N. Hara, Direct Observation of Pit Initiation Process on Type 304 Stainless Steel, Materials Transactions **55** (2004) 857–860.

Figures & Captions

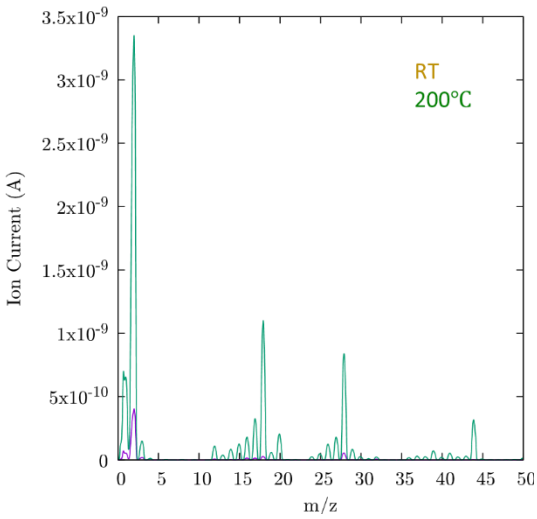

Figure 1. Ion current measured with quadrupole mass spectrometer before DIET measurement at room temperature (red) and at 473 K (green).

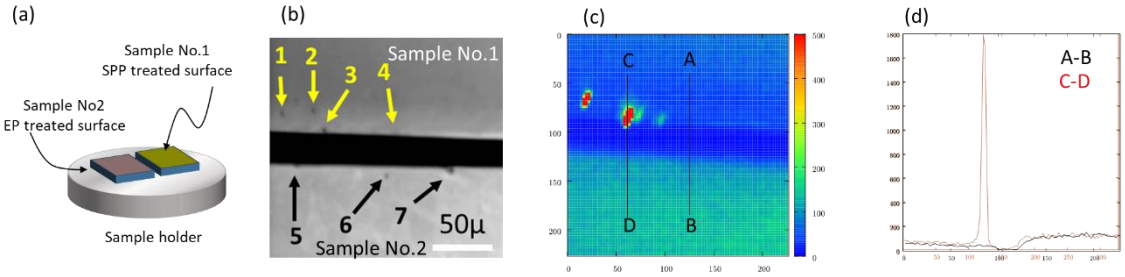

Figure 2. SEM image and DIET measurement of FF-SPP–treated and electropolished (EP) surfaces.
(a) Schematic diagram of samples and sample holder. **(b)** SEM image of the two samples mounted together on one holder. The black area in the middle is the empty space between the two samples. Sample No. 1 and sample No. 2 were subjected to EP under the same conditions. Sample No. 1 underwent FF-SPP treatment after EP. Arrows with numbers indicate small defects on the surface. **(c)** DIET map at 200 °C of the same area as shown in (b). **(d)** Hydrogen desorption profile along line A–B and line C–D in (c)

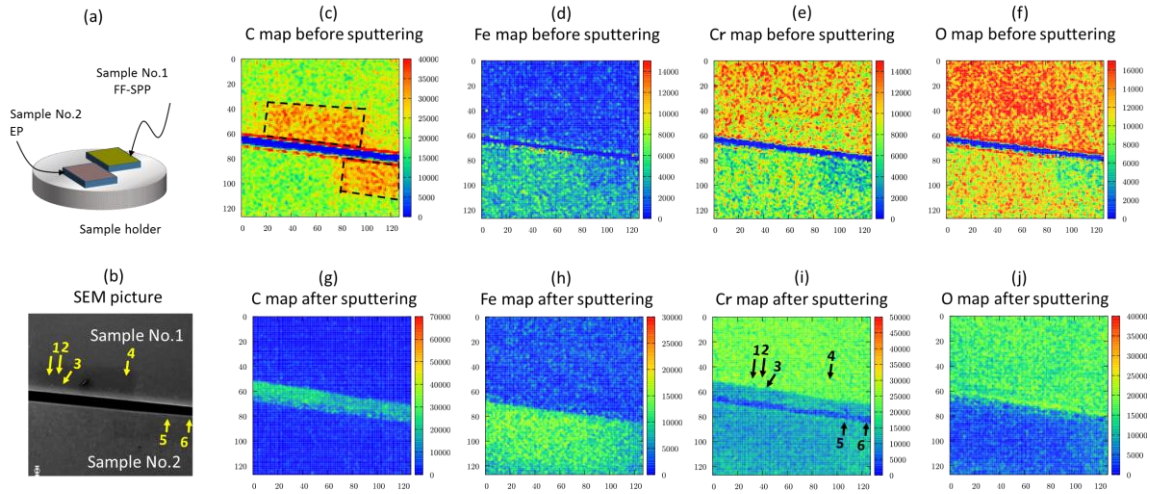

Figure 3. Distribution of surface atoms measured by Auger electron spectroscopy (AES).
(a) Schematic diagram of samples and sample holder in the AES machine. **(b)** SEM image of the two samples. **(c–j)** Auger maps of carbon, iron, chromium, and oxygen. Carbon on the surface was removed by sputtering with low-speed argon ions. **(c–f)** Surfaces before carbon removal. **(g–j)** Surfaces after carbon removal. In the Cr map **(i)** we marked the locations of defects 1 and 3 with arrows.

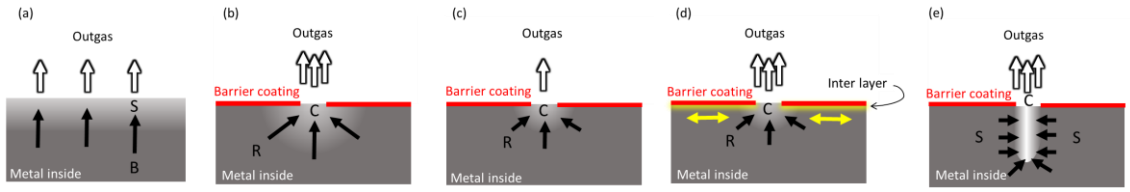

Figure 4. **(a)** Schematic of outgassing from metal surface. **(b)** Outgassing from the surface with a barrier coating, assuming diffusion of hydrogen as a gas in a sealed container. **(c)** Outgassing assuming diffusion of hydrogen as molecular flow. **(d)** Outgassing assuming diffusion of hydrogen outgassing with another diffusion path. **(e)** Assuming hydrogen outgassing from a space under the holelike defect. Hydrogen diffuses from the metal to the space.